



IJRASET

International Journal For Research in
Applied Science and Engineering Technology



INTERNATIONAL JOURNAL FOR RESEARCH

IN APPLIED SCIENCE & ENGINEERING TECHNOLOGY

Volume: 10 **Issue:** VI **Month of publication:** June 2022

DOI: <https://doi.org/10.22214/ijraset.2022.44217>

www.ijraset.com

Call:  08813907089

E-mail ID: ijraset@gmail.com

Blade Design and Performance Analysis of Wind Turbine

Rahul Vaidhye¹, Prof. Ritesh Banapurkar², Pravin Vasram Jadhav³

^{1, 2, 3}Abha Gaikwad-Patil College of Engineering (AGPCE Mohgaon Nagpur)

Abstract: This paper reviews the design optimization of wind turbine blades through investigating the design methods and analyzing the performance of the blades. The current research work in this area include wind turbine blade geometric design and optimization, aerodynamics analysis, wind turbine blade structural design and dynamics analysis. Blade geometric design addresses the design parameters, including airfoils and their aerodynamic coefficients, attack angles, design tip speed ratio, design and/or rated wind speed, rotor diameter, blade aerodynamic shape with chord length and twist distributions, so that the blade achieves an optimum powerperformance. The geometry of the blade is an aerodynamic shape with nonlinear chord and twist distribution, which can be obtained based on the BEM theory with respect to given aerofoil with known aerodynamic coefficients. In terms of blade aerodynamics analysis, there are four types of aerodynamic models which can be used to predict the aerodynamic performance of blades, including blade element momentum (BEM) model, lifting panel and vortex model, actuator line model, and computational fluid dynamics (CFD) model. Among the four, computational fluid dynamics (CFD) model has been used to calculate the aerodynamic effect on the bladeairfoil. Critical Reynolds number and constant wind speed has been considered during analysis under different turbulence models Viz, spallart-almaras, k-epsilon, invicid flow. During investigation it is observed that only k- epsilon showed efficient results than others and 14 degree angle of attack (AOA) is the optimum value at which there is much lift coefficient and minimum drag.

Keywords: Angle of attack α , aerodynamic coefficients c_l & c_d , blade aerofoil, turbulence models etc.

I. INTRODUCTION

The wind is solar power in mechanical form. A small part (around 2 %) of the energy of solar radiation on Earth is converted into kinetic energy of flowing air, the wind. Wind's velocity and direction depend on the imposed pressure gradients, plus certain other forces, plus the local geography. The wind is a free-flowing fluid stream. The energy extraction device (of any type) is submersed into this stream and can convert only a certain amount from the total available energy in the fluid stream, not all of it. Energy conversion from free-flowing fluid streams is limited because energy extraction implies decrease of fluid velocity (decrease of kinetic energy of the stream), which cannot fall down to zero, the stream should continue traveling and cannot stop entirely. Also, the turbine is an obstruction to the fluid flow. Some fluid may not pass through the turbine and may simply flow around it. The most common type of lift-force wind turbines is the horizontal axis wind turbine - HAWT. The rotor axis lies horizontally, parallel to the air flow. The blades sweep a circular (or slightly conical) plane normal to the air flow, situated upwind (in front of the tower) or downwind (behind the tower). The main advantage of HAWTs is the good aerodynamic efficiency (if blades are properly designed) and versatility of applications¹. Their main disadvantage is that the tower must support the rotor and all gearing and electricity

Generation equipment standing on top of it, plus the necessity of yawing to face the wind. A wind turbine transforms the kinetic energy in the wind to mechanical energy in a shaft and finally into electrical energy in a generator. The maximum available energy, P_{max} , is thus obtained if theoretically the wind speed could be reduced to zero: $P = 1/2 m V^2 = 1/2 \rho A V^3$ where m is the mass flow, V is the wind speed, ρ the density of the air and A the area where the wind speed has been reduced. The equation for the maximum available power is very important since it tells us that power increases with the cube of the wind speed and only linearly with density and area. The available wind speed at a given site is therefore often first measured over a period of time before a project is initiated.

In practice one cannot reduce the wind speed to zero, so a power coefficient C_p is defined as the ratio between the actual power obtained and the maximum available power as given by the above equation. A theoretical maximum for C_p exists, denoted by the Betz limit^{2,3}, $C_p \text{ max} = 0.593$. Modern wind turbines operate close to this limit, with C_p up to 0.5, and are therefore optimized.

Statistics have been given on many different turbines sited in Denmark and as rule of thumb they produce approximately 1000kWh/m²/year. However, the production is very site dependent and the rule of thumb can only be used as a crude estimation and only for a site in Denmark. Sailors discovered very early on that it is more efficient to use the lift force than simple drag as the main source of propulsion. Lift and drag are the components of the force perpendicular and parallel to the direction of the relative wind respectively. It is easy to show theoretically that it is much more efficient to use lift rather than drag when extracting power from the wind. All modern wind turbines therefore consist of a number of rotating blades looking like propeller blades. If the blades are connected to a vertical shaft, the turbine is called a vertical-axis machine, VAWT, and if the shaft is horizontal, the turbine is called a horizontal-axis wind turbine, HAWT. For commercial wind turbines the mainstream mostly consists of HAWTs; the following text therefore focuses on this type of machine. A HAWT as sketched in Figure 1 in which Gorban, A. N. (2001)⁵ describes in terms of the rotor diameter, the number of blades, the tower height, and the rated power.

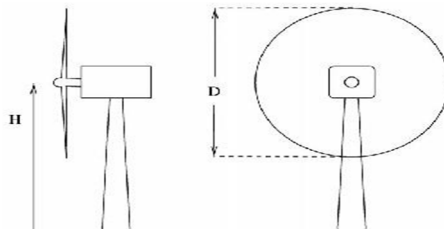


Figure 1 Horizontal Axis wind Turbine [NREL]

II. GOVERNING EQUATIONS

Law of conservation of mass i.e., mass can neither be created nor destroyed. This fundamental principal when applied to model of fluid yields the continuity equation.

$$\frac{dm}{dt} = 0$$

In differential form:

$$\frac{\partial \rho}{\partial t} + \nabla \cdot (\rho \vec{V}) = 0$$

Law of conservation of momentum i.e., momentum can be changed by application of forces and is obtained from Newton's Second law of motion.

$$\frac{d(m\vec{V})}{dt} = \sum \vec{F}$$

In differential form:

$$\frac{\partial(\rho \vec{V})}{\partial t} + \nabla \cdot (\rho \vec{V} \vec{V}) = -\nabla p + \nabla \cdot (\vec{\tau}) + \rho \vec{g} + \vec{F}$$

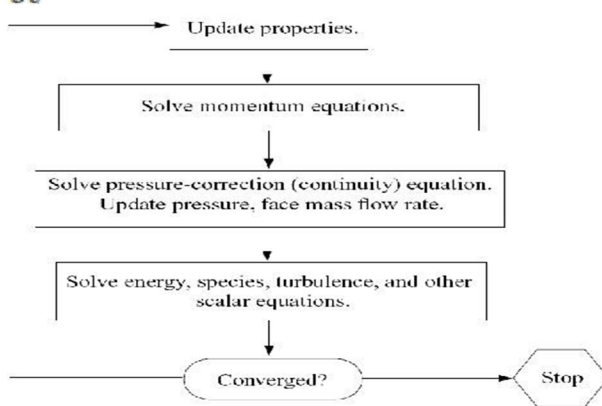


Figure 2 Segregated solution methods⁴

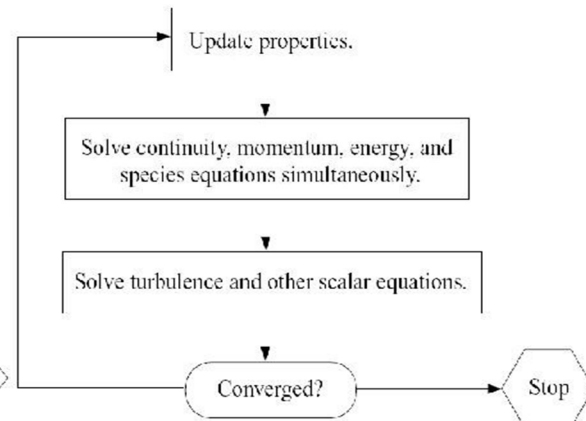
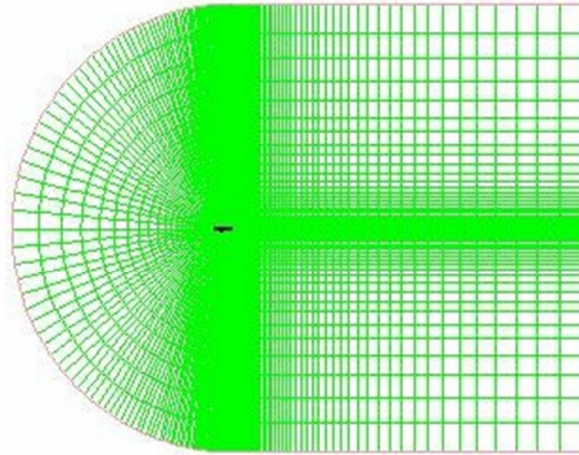


Figure 3 Coupled solution methods⁵

III. MESH GENERATION



Source: Mesh Generation⁶.

A. Fluent Simulation

The geometries and mesh are imported into FLUENT, and the system and environment properties set. “PRESTO!” and “Double precision” is selected as system parameters, ensuring adequate accuracy. FLUENT has single precision as default, but for these simulations an accurate solution is requested. The residuals for the different turbulence model variables were set to 10^{-8} and the iteration max count to 1000. The simulation process could also be halted or stopped if the CL or CD seemed to have stabilized properly. After the boundary type of the computational domain and the model are specified in gambit the mesh is exported to fluent for further simulation. Before starting a simulation in fluent, the mesh has to be checked and scaled, also defining the boundary conditions, other parameters and initial conditions. This includes the choice of compressibility, viscosity, laminar or turbulent flow, steady or time dependent flow. The various numerical methods and simulation parameters set in fluent are as under:

B. Initial Boundary Condition

In the computational flow domain the boundary condition of translational movement to the ground is given in the same direction and magnitude as the incoming air velocity, i.e. (50 m/s). The airfoil is set to the walls properties.

- 1) Inlet Velocity = 50m/s
- 2) Outlet Pressure = 0 Pascal
- 3) Turbulence specification method=K and epsilon/Spalart-Almiras/IncidTurbulent Kinetic Energy = $0.001\text{m}^2/\text{s}^2$
- 4) Turbulent Dissipation Rate = $0.0001\text{m}^2/\text{s}^2$

IV. MATERIAL

For CFD analysis of the flow over the S809 series airfoil of a wind turbine model, the continuum used is air and its properties are

- I. Density = 1.225 kg/m³
- II. Specific Heat (C_p) = 1006.43 j/kg-k
- III. Thermal Conductivity = 0.0242 w/m-k
- IV. Viscosity = 1.7894e-05 kg/m-s
- V. Molecular Weight = 28.966 kg/kgmol

A. Operating Conditions

- I. Atmospheric Pressure = 101325 Pascal
- II. Temperature = 288.16 Kelvin

B. Model Parameters

- I. Solver = Segregated
- II. Viscous = k-ε/Spalart-Allmaras/Inviscid
- III. Formulation = Implicit
- IV. Space = 3D
- V. Wall Treatment = Standard Wall Functions
- VI. Time = Unsteady, 1st Order Implicit
- VII. Time Stepping Method = Fixed
- VIII. Velocity Formulation = Absolute
- IX. Gradient Option = Cell Based
- X. Convergence Criteria = 1e-3

C. Discretization Scheme

The discretization Scheme applied for solving the flow and turbulence equation are as under:

- I. Pressure = Standard
- II. Momentum = Second Order Upwind
- III. Turbulence Kinetic Energy = Second Order Upwind
- IV. Turbulence Dissipation Rate = Second Order Upwind
- V. Pressure Velocity Coupling = SIMPLE

D. Viscosity Models

Considering vortex shedding and boundary layer separation for airfoils and wings, this simulation will have to deal with turbulent flows.

The chaotic nature of turbulent flow makes it very expensive to compute velocities for all points in space. RANS is the opposite to DNS which is the analytic direct simulation of the governing equations, and use a statistical and averaged approach to find the flow behavior⁷. The reason for using RANS models is that small vortices – in turn very expensive to solve - are removed by averaging the flow.

A crucial point is selecting a viscous model, and in FLUENT there are several options. There are fundamental differences to the different models, and may be used for different types of flows. In this project, the viscous models *k-ε* and *Spalart-Allmaras* are used. Both are RANS models. *k-ε* is a 2-equation model, whilst *Spalart-Allmaras* (S-A) is a newer 1-equation model and is well-suited for external flows as with the S809 series airfoil.

V. RESULTS & DISCUSSIONS

It is observed that the results change on the basis of airfoil geometry⁸. Present results depict the lift and drag coefficients are showing monotonic increase/decrease with respect to the angle of attack (AOA).

The aim of the simulations has been to determine the flow field around the airfoil of the wind turbine responsible for the buildup of forces acting on the airfoil. In this investigation of flow around the simplified airfoil shape that included different viscosity models at constant Reynolds number.

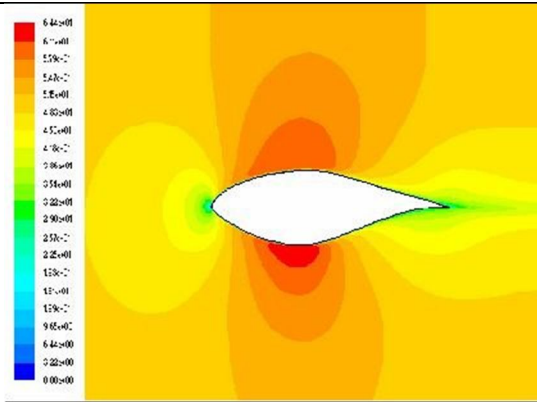
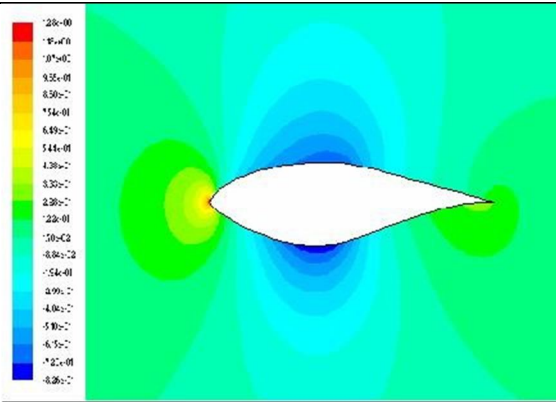
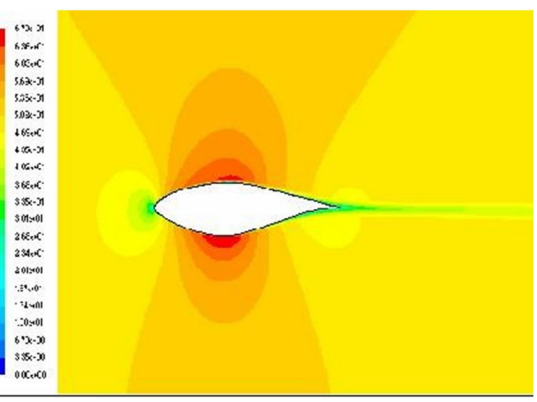
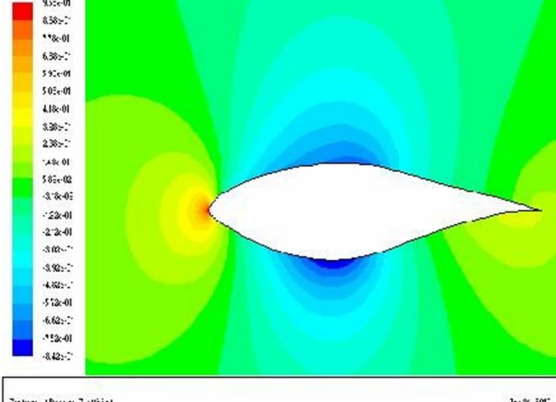
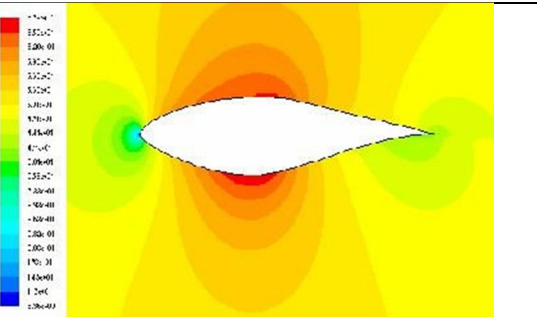
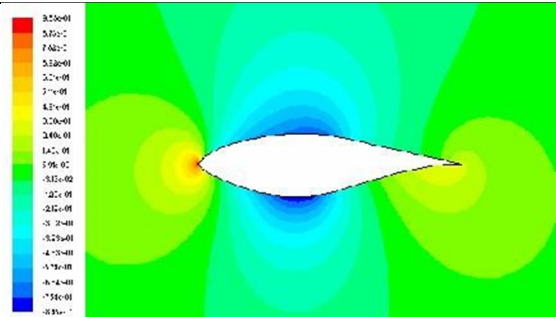
The range of the results varies with respect to the viscosity models and with the function of angle of attack with different airfoil geometries.

All the analysis was performed using turbulence models like K-epsilon, Spalart-Allmaras and Viscous for the simulation S809 series airfoil at various angle of attacks (AOAs) starting from -2.23 to 20 degrees respectively. For quantitative validation the experimental Wind Tunnel Profile Coefficients data was taken as a basis. The CFD analysis of the flow over an airfoil of a simplified section gave relatively good agreement with the experiments.

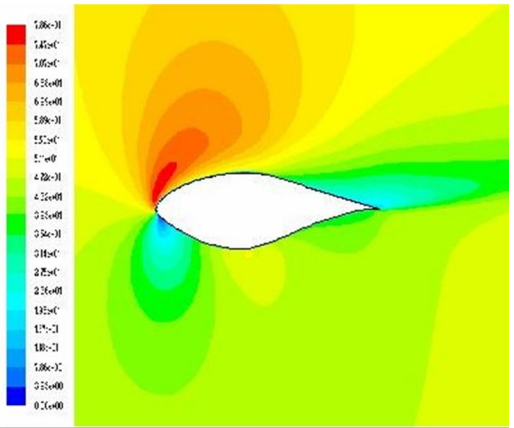
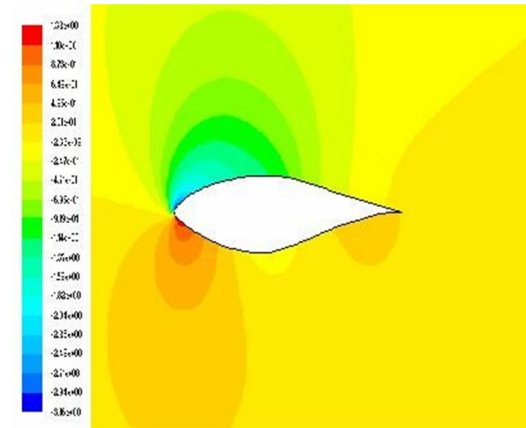
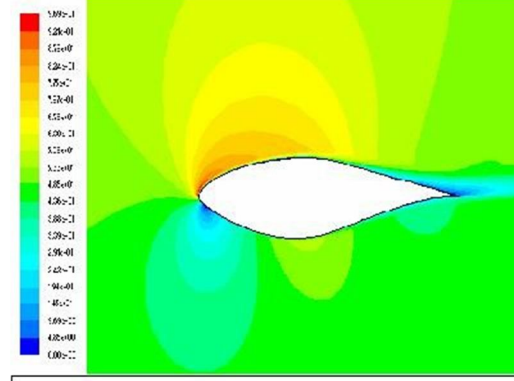
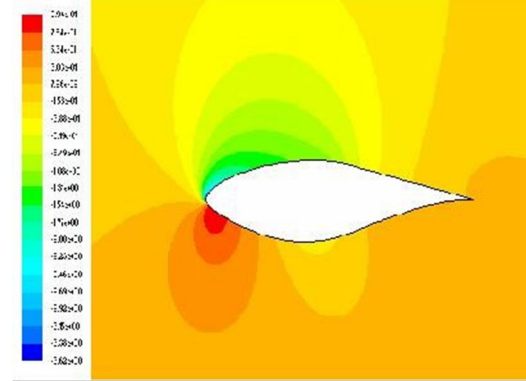
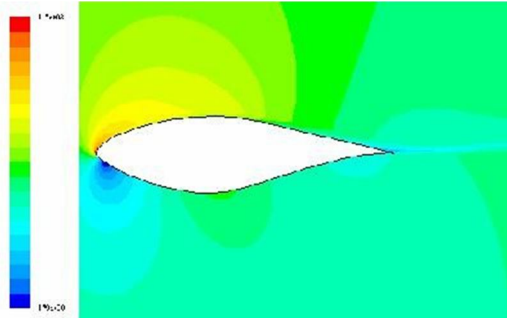
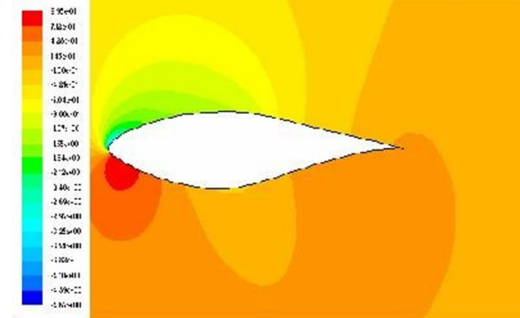
VI. RESULTS

The following table shows the different contour outputs from the simulations. Viscous models *k-ε*, *Spalart-Allmaras* and *Inviscid* are compared in separate rows as a function of Angle of attacks (AOAs).

Angle of Attack, $\alpha = 0^\circ$

Model	Velocity distribution	Pressure distribution
K-ε	 <p>Contours of Velocity Magnitude [m/s]</p> <p>July 26, 2022 FLUENT 6.2.3d (32-bit) x64</p>	 <p>Contours of Pressure Coefficient</p> <p>July 26, 2022 FLUENT 6.2.3d (32-bit) x64</p>
S-A	 <p>Contours of Velocity Magnitude [m/s]</p> <p>July 26, 2022 FLUENT 6.2.3d (32-bit) x64</p>	 <p>Contours of Pressure Coefficient</p> <p>July 26, 2022 FLUENT 6.2.3d (32-bit) x64</p>
Inviscid	 <p>Contours of Velocity Magnitude [m/s]</p> <p>July 26, 2022 FLUENT 6.2.3d (32-bit) x64</p>	 <p>Contours of Pressure Coefficient</p> <p>July 26, 2022 FLUENT 6.2.3d (32-bit) x64</p>

Angle of Attack, $\alpha = 14^\circ$

Model	Velocity distribution	Pressure distribution
K-ε	 <p>Contours of Velocity Magnitude (m/s)</p> <p>July 21, 2020 FLUENT 12.1 (64-bit) x64: 64-bit</p>	 <p>Contours of Pressure Coefficient</p> <p>July 21, 2020 FLUENT 12.1 (64-bit) x64: 64-bit</p>
S-A	 <p>Contours of Velocity Magnitude (m/s)</p> <p>July 21, 2020 FLUENT 12.1 (64-bit) x64: 64-bit</p>	 <p>Contours of Pressure Coefficient</p> <p>July 21, 2020 FLUENT 12.1 (64-bit) x64: 64-bit</p>
Inviscid	 <p>Contours of Velocity Magnitude (m/s)</p> <p>July 21, 2020 FLUENT 12.1 (64-bit) x64: 64-bit</p>	 <p>Contours of Pressure Coefficient</p> <p>July 21, 2020 FLUENT 12.1 (64-bit) x64: 64-bit</p>

A. Lift Coefficient

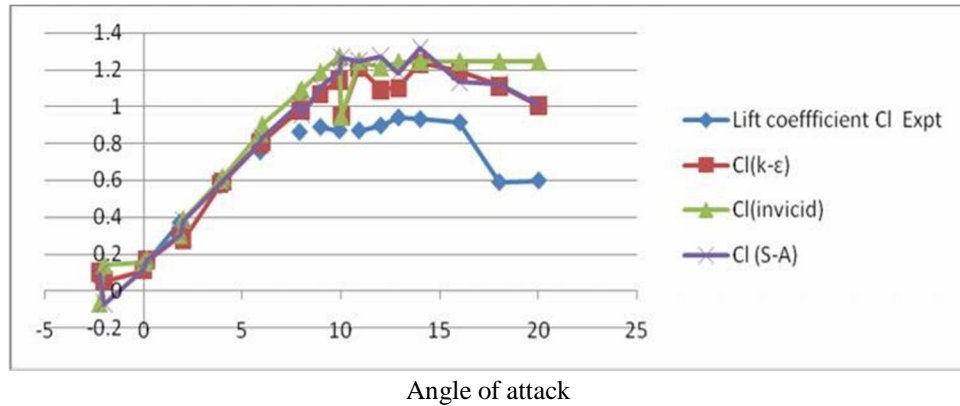


Figure 4: Graphical Interpretation for comparison between Computed lift coefficient CFD Based and Experimental at various viscosity Models.

B. Drag Coefficient

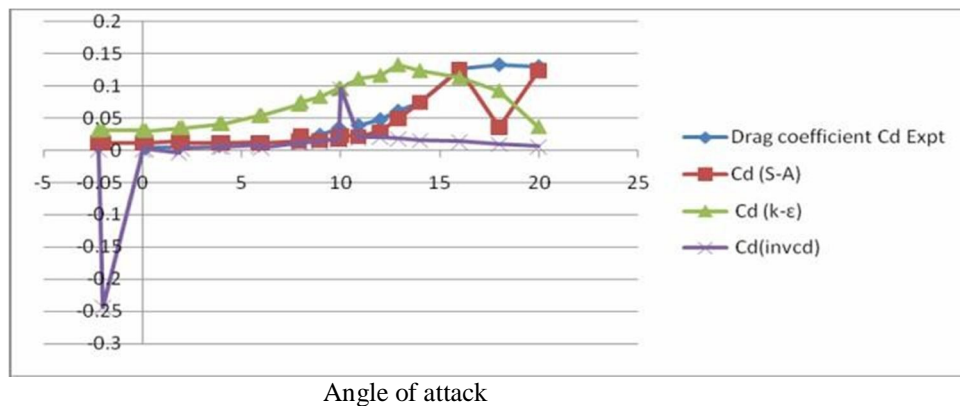


Figure 5 : Graphical Interpretation for comparison between Computed Drag coefficient CFD Based and Experimental at various viscosity Models.

Comparing the graphs, contours a clear correlation has been found between the experimental data and the simulations. All the different turbulent models follow the slope of the experimental data until $\sim 8^\circ$. Only the Spalart-Allmaras model properly identifies the stall angle at 14° .

For C_d only $k-\epsilon$ shows satisfactory correlation to the experimental data. Considering the quite similar performance in determining C_l , $k-\epsilon$ seems like the overall best turbulence model to use.

VII. CONCLUSION

Lab experiments and CFD simulations has proven that for this particular S809 series airfoil, the most effective angle of attack is at 14° . From 6° to 14° the C_L will be above a value of 1, and from 3° to 14° the ratio L/D will be over 1, in other words; within this range there will be effective use of the airfoil. The good correlations between wind tunnel data and CFD simulations encourage that future modification on airfoil designs shall be investigated in simulation software⁹. Though, it is emphasized that wind tunnel experiments must still be done to validate the accuracy of the evolving designs and computer models. The CFD software used in this report has limitations in terms of flexibility in meshing. Acquiring different software with more mesh options, or just a specific meshing software, is therefore recommended. Ideally there should have been carried out simulations on both high and low Reynolds Numbers. It is difficult to acquire the necessary data for this, and due to time constraints only one Re is being investigated here. It is recommended that future work on the same subject acquire experimental data for more than one velocity. Future work should also consider using *Spalart-Allmaras* and $k-\omega$ instead of $k-\epsilon$, which may have a better result on flow close to boundary layers



REFERENCES

- [1] Corbus, D., (2005) "Comparison between Field Data and NASA Ames Wind Tunnel Data," Technical report for the National Renewable Energy Laboratory, TP-500- 38285.
- [2] White, F.M., (1988) Fluid Mechanics, 2nd Edition, McGraw-Hill, sangopore.
- [3] Madsen, H.A., Mikkelsen, R.,ye, S., Bak, C., and Johansen, J., (2007) "A Detailed Investigation of the Blade Element Momentum (BEM) model based on analytical and numerical results and proposal for modification of the BEM model," The Science of Making Torque from Wind, Journal of Physics: Conference Series 75.
- [4] Simms, D., Schreck, S., Hand, M., and Fingersh, L.J., (2001) "NREL Unsteady Aerodynamics Experiment in the NASA-Ames Wind Tunnel: A Comparison of Predictions to Measurements," Technical report for the National Renewable Energy Laboratory, TP-500-29494.
- [5] Gorban, A. N., (2001) "Limits of the Turbine Efficiency for Free Fluid Flow," Journal of Energy Resources Technology, Vol. 123, pp. 311 – 317.
- [6] Wolfe, W.P., and Ochs., S.S., (1997) "CFD Calculations of S809 Aerodynamic Characteristics," American Society of Mechanical Engineers wind energy symposium, Reno, NV (United States).
- [7] Leishman J G and Beddoes T S. (1989) A semi-empirical model for dynamic stall. Journal of the American Helicopter Society, 34(3):3.
- [8] Laursen, J., Enevoldsen, P., and Hjort, S., (2007) "3D CFD Quantification of the Performance of a Multi-Megawatt Wind Turbine," The Science of Making Torque from Wind, Journal of Physics:Conference Series 75
- [9] Najar, F.A(2010) Thesis submitted at National institute of Technology, Srinagar in 2010, Design and analysis of wind turbine blade S809 series airfoil, using CFD as a tool.
- [10] Jonkman, J.M., (2003) "Modelling of the UEA Wind Turbine for Refinement of FAST_AD," Technical report for the National Renewable Energy Laboratory, TP- 500-34755.



10.22214/IJRASET



45.98



IMPACT FACTOR:
7.129



IMPACT FACTOR:
7.429



INTERNATIONAL JOURNAL FOR RESEARCH

IN APPLIED SCIENCE & ENGINEERING TECHNOLOGY

Call : 08813907089  (24*7 Support on Whatsapp)